agriculture

MDPI

Article

Performance Evaluation of Biomimetic-Designed Rotary Blades for Straw Incorporation in an Intensive Tillage System

Xinxin Chen [1,†], Gaoming Xu [2,*,†], Xiaoyu Zhang [2], Weichao Tan [2], Qishuo Ding [3] and Ahmad Ali Tagar [4]

[1] College of Agricultural Engineering, Jiangsu University, Zhenjiang 212001, China; xxchen@ujs.edu.cn
[2] College of Intelligent Manufacturing and Equipment, Jiangmen Polytechnic, Jiangmen 529090, China
[3] Key Laboratory of Intelligent Agricultural Equipment of Jiangsu Province, College of Engineering, Nanjing Agricultural University, Nanjing 210031, China
[4] Department of Farm Power and Machinery, Faculty of Agricultural Engineering, Sindh Agriculture University, Tandojam 70060, Pakistan
* Correspondence: 2020212002@stu.njau.edu.cn
† These authors contributed equally to this work.

Abstract: A rotary tiller is a common tillage tool for straw incorporation in an intensive tillage system. However, rotary tillage for seedbed preparation in dense-straw mulching conditions experiences high torque and poor performance of straw incorporation. Nowadays, a great deal of studies have been focused on mimicking the morphological features of low-resistance animals to improve the performance of soil-engaging tools. Accordingly, the present study investigated the performance of three C-type rotary blades (i.e., conventional, serrated, and biomimetic) under three straw lengths (50, 100, and 150 mm) for incorporation of straw into the field using an in situ field tillage testing bench. Compared to the conventional and serrated blades, the biomimetic blade had lower straw displacement (decreased by an average of 50 mm and 7 mm, respectively), higher straw burying rate (increased by an average of 5.2% and 7.8%, respectively), better straw distribution (decreased by an average of 9.1% and 10.4% on the coefficient of variation, respectively), as well as lower torque and power (decreased by an average of 3.3 N·m and 4.4 N·m, respectively) under all straw lengths. The improved performance of the biomimetic blade could be attributed to the fact that its typical teeth configuration was designed by mimicking the smooth arc of the mole-rat's claw. These results demonstrated that the biomimetic-designed blade could be a better option for incorporating dense straw into the field conditions.

Keywords: biomimetic design; rotary blade; straw displacement; straw burying; straw distribution; torque and power

Citation: Chen, X.; Xu, G.; Zhang, X.; Tan, W.; Ding, Q.; Tagar, A.A. Performance Evaluation of Biomimetic-Designed Rotary Blades for Straw Incorporation in an Intensive Tillage System. *Agriculture* **2024**, *14*, 1426. https://doi.org/10.3390/agriculture14081426

Received: 2 July 2024
Revised: 9 August 2024
Accepted: 21 August 2024
Published: 22 August 2024

1. Introduction

In recent years, the attention focused on intensive, high-yield agriculture has been substantial as it enhances crop productivity, optimizes resource utilization efficiency, and elevates labor efficiency [1–5]. Nevertheless, the high yield of crops is accompanied by a high output of crop straw, resulting in a significant accumulation of residues in the field after harvesting, which hinders planting operations, seed germination, and early plant development [6]. Consequently, it is imperative to explore a high-performance tillage tool to address the issue of excessive crop residue in the field.

In the intensive rice–wheat rotational system implemented in eastern China, the limited annual heat resource requires the timely preparation of seedbeds for the next crop after harvesting the previous crop [7]. Excessive crop residues on the soil surface further complicate seedbed preparation, resulting in the failure of timely planting of the subsequent crop [8,9]. Farmers' typical practice of conventional tillage (straw incorporation passes using moldboard plows) for seedbed preparation is time and energy-intensive. In comparison, the use of rotary tillers has demonstrated relatively high working efficiency

and residue incorporation capacity, as well as lower energy requirements [10,11]. However, conventional rotary blades working in dense-residue mulched tillage incur high resistance with inflated energy demands. Moreover, plenty of residues after tillage are distributed in the sowing depth layer of 0–50 mm, which will also block machines, overhead seed placement, and delay seed germination [12,13]. Hence, it is imperative to investigate a high-performance tillage tool that can properly incorporate straw into the field with reduced power requirement in a considerably short time period.

Despite the recognition of the significance of high-performance tillage tools in the intensive rice–wheat rotational system, as emphasized in numerous studies [7,14], the development of an effective method for designing soil-cutting and residue-handling tools remains limited. Biomimetic design, a method that leverages biological systems for the creation of technical equipment, has garnered substantial attention for its potential to enhance and optimize tillage tools [15]. In nature, there are a multitude of low-resistance animals, such as moles, badgers, and pangolins. These animals have undergone a substantial degree of adaptation to their natural environment, as documented by numerous studies [16–18]. Hence, high-performance tillage tools can be designed and manufactured by simulating the structures of these animals.

Many studies have been undertaken to evaluate the potential of biomimetic designs inspired by low-resistance animals in enhancing the performance of soil-engaging tools [19–22]. Song et al. [23] conducted an investigation into a subsoiler mimicking the claw features of the mole-rat, which achieved a 20.0% increase in soil looseness at various tillage depths when compared to the conventional subsoiler. Sun et al. [24] devised a ditcher blade mimicking the claw of a bear and found that the tillage resistance, power, and specific energy consumption were comparatively lower compared to that of the conventional ditcher blade. Furthermore, Yang et al. [25] studied a soil-engaging tool simulating the claws of a mole's hand and indicated that the ratio of soil rupture distance was decreased by approximately 19.6% in comparison to the traditional blades when evaluated at varying rake angles.

Although numerous studies have mimicked the biomimetic designs, no tool has been specifically designed for crop residue incorporation in dense straw conditions. Previous research has primarily focused on improving soil–tool interaction by mimicking the features of biological systems rather than the soil–straw–tool interactions. The soil–tool interaction typical in intensive rice–wheat rotation systems has upgraded to soil–straw–tool interaction by excessive crop residues [26]. Thus, the current study aims to examine a high-performance tool based on biomimetic designs to effectively handle crop residue in dense straw conditions. The objectives of the study were to (i) evaluate and compare the effect of three different types of rotary blades (i.e., conventional, serrated, and biomimetic) on straw displacement under three straw lengths (i.e., 50, 100, and 150 mm) and (ii) study and compare the effect of three different types of rotary blades (i.e., conventional, serrated, and biomimetic) on straw burying, straw distribution, and energy consumption under three straw lengths (i.e., 50, 100, and 150 mm) in an intensive rice–wheat rotation system.

2. Materials and Methods

2.1. Description of the Test Site

A field experiment was carried out in November 2021 at a Research Farm of Nanjing Agricultural University in Jiangsu Province, utilizing a paddy field with abundant crop residues post-harvest. The test site has a history of being utilized for the implementation of the rice–wheat rotation system. The soil of the experimental site was classified as clay loam (38.86% clay, 39.84% silt, and 21.30% sand, respectively). Table 1 presents the soil physical, including cone index, soil moisture content, dry bulk density, and straw parameters, such as length, wet density, and dry density before tillage operations.

Table 1. Soil properties and straw parameters before tillage operations.

Type	Parameters	Value
Soil	Cone index	673, 984, 961 kPa at 50, 100, and 150 mm depths, respectively
	Moisture content	23.4, 23.9, 24.5% at depth of 0–50, 50–100, and 100–150 mm, respectively
	Dry bulk density	1.29 g cm^{-3}
Straw	Straw length	0–150 mm
	Wet density	8051 kg ha^{-1}
	Dry density	3972 kg ha^{-1}
	Moisture content	50.6% (wet basis)

2.2. Designs of Rotary Blades

The biomimetic blade was designed and developed by mimicking the claw profile of a mole-rat, as proposed by Tong et al. [27]. The fitting arc was used to simulate the geometrical characters of the middle three toes of the mole-rat, but the shape of the middle three toes is identical. Hence, the fourth toe of mole-rat was employed in the study. The arc was amplified 12 times and reverse-engineered into a blade with five identical soil-engaging teeth in the frontal cutting edge, as illustrated in Figure 1. The total length of the front cutting edge of the blade was 60 mm; hence, five reverse arc (to hold the straw and move more straw backward in an ordered manner) teeth of the mole-rat with a diameter of 12 mm (slightly larger than the diameter of a single straw) were arranged on the front cutting edge with a total length of 60 mm to reduce soil-cutting resistance and improve the efficiency of straw incorporation.

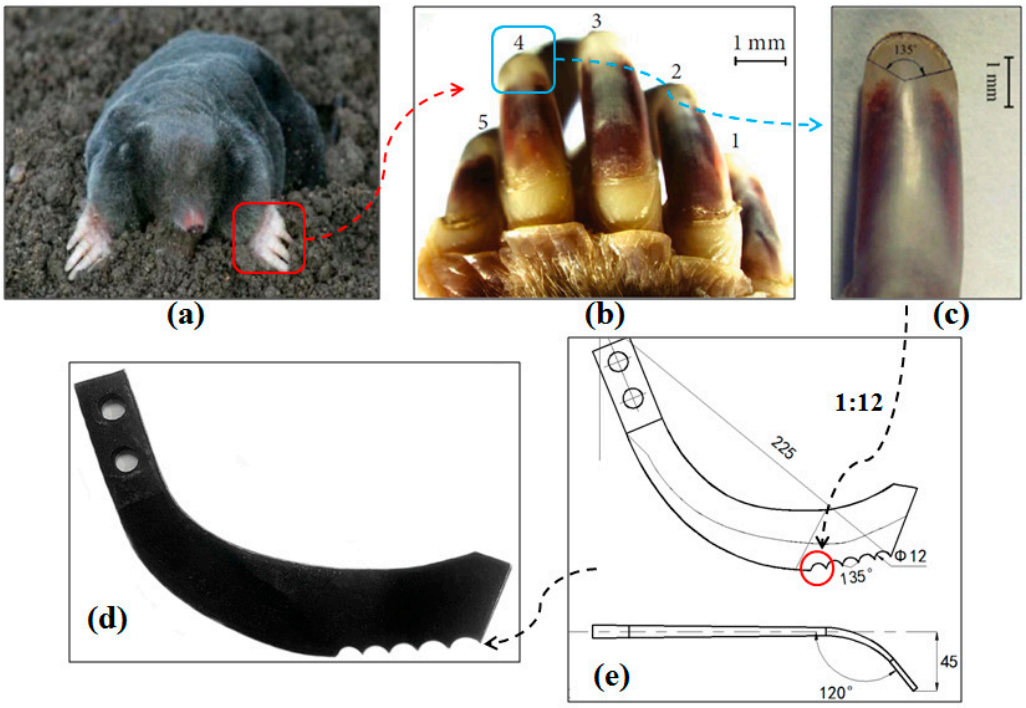

Figure 1. (**a**) A mole, (**b**) a mole's toe-claws, (**c**) picture of a mole's claw, (**d**) developed biomimetic blade, (**e**) configurations of the biomimetic blade reverse-engineered from the mole's claw.

The design configurations of the conventional blade and serrated blade are shown in Figure 2.

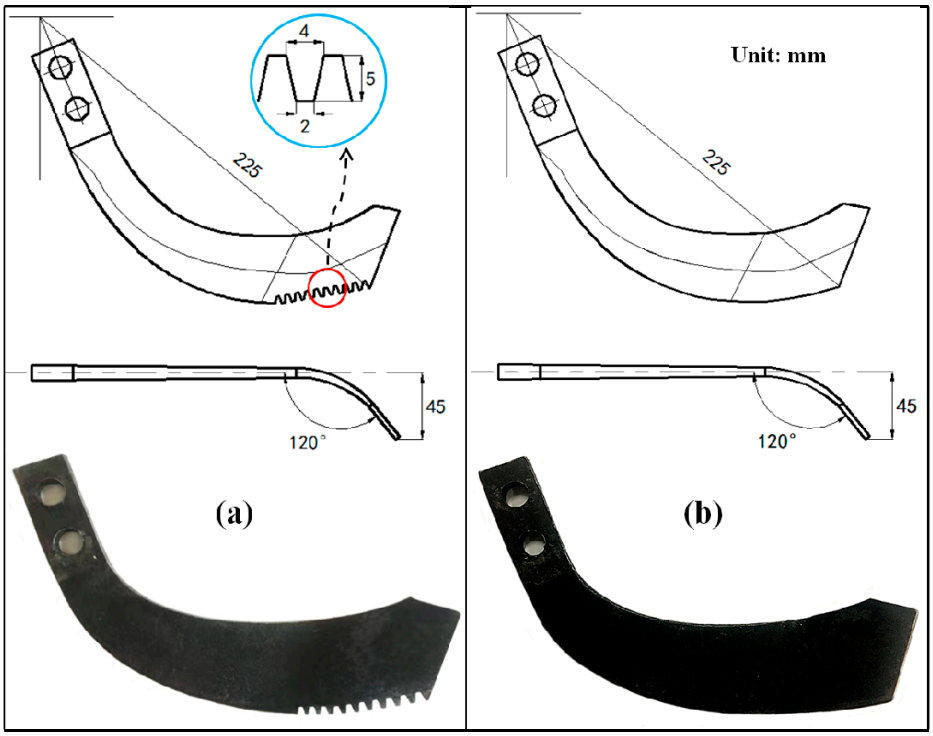

Figure 2. (**a**) Design structure of the serrated blade, (**b**) an unmodified conventional blade.

The blades (i.e., conventional, serrated, and biomimetic) were obtained from the local markets, but the configurations of serrated and biomimetic blades were not identical to those of the conventional blade. Therefore, the serrated and biomimetic blades were machined to give similar configurations using a CNC wire-cut machine (DK7763, Baomade Electromechanical, Suzhou, China) to evaluate the performance of the blades. The blades were designed using Auto CAD 2016 software. The specifications of the blades are listed in Table 2.

Table 2. Specification of the experimental blades.

Specification	Blade Design		
	Conventional Blade	**Serrated Blade**	**Biomimetic Blade**
Rotary radius, mm	225	225	225
Cutting width, mm	45	45	45
Bend angle, °	120	120	120
Blade thickness, mm	25	25	25
Number of teeth	—	10	5
Tooth base width, mm	—	4	11
Tooth height, mm	—	5	4

2.3. Description of the In Situ Test Rig

An in situ test rig developed at Nanjing Agricultural University, China, was used to perform the field experiment (Figure 3). The rig is 8000 mm long and 1800 mm wide. This rig consists of multiple components, including a diesel-driven generator, a movable carriage unit, a lifting system, a pulling system, a control and operating system, and a data collection system. The movable carriage unit moves along twin guide rails at adjustable speeds ranging from 0.05 to 1 m s^{-1} and is controlled by a wireless operating handle, which can move forward and backward and up and down. The rig is powered by a 13.5 kW diesel-driven generator and has a 7.5 kW rotary motor for adjustable tillage speed from 0 to 600 rpm. A torque sensor is attached to the driving shaft to acquire data, and the three

types of blades (conventional, serrated, and biomimetic), including 7 left blades and 7 right blades, are installed at the center on a 0.8 m shaft in a double spiral arrangement.

Figure 3. Overview of the in situ test rig: 1. Column lifting motor, 2. Control system, 3. Power connection interface, 4. Carriage unit, 5. Pulling motor, 6. Data collection computer, 7. Data collection unit, 8. Diesel-driven generator, 9. Power transmission cable, 10. Operating handle, 11. Rotary blade, 12. Driving shaft, 13. Torque sensor, 14. Drawing chain, 15. Guide rail, 16. Force sensor, 17. Power screw and motor, 18. Rotary motor.

2.4. Experimental Design

The length range of residual straw in the field is 0–150 mm; this study refers to a previous study [26] and uses three straw lengths of 50, 100, and 150 mm to represent the overall situation of straw. This study consisted of two experiments: (i) To evaluate and compare the effect of three different types of rotary blades (i.e., conventional, serrated, and biomimetic) on straw displacement under three straw lengths (i.e., 50, 100, and 150 mm). To obtain the data on straw displacement, straw was painted with red and blue colors to represent longitudinal and lateral displacements, respectively, as illustrated in Figure 4a. (ii) To study and compare the effect of three different types of rotary blades (i.e., conventional, serrated, and biomimetic) on straw burying, straw distribution, and energy consumption under three straw lengths (i.e., 50, 100, and 150 mm). The previous crop residues were removed from the field surface. Straw was chopped in three different lengths (i.e., 50, 100, and 150 mm), painted with red color, and then spread on the field surface manually at the rate of 8051 kg ha^{-1} [12], as shown in Figure 4b.

The experimental field was divided into 36 plots (5 m × 2 m) using a single-factor randomized block design. Each treatment was replicated three times. The operational parameters, such as tillage depth (100 mm), rotary speed (280 rpm), and forward speed (0.5 m s^{-1}), were set according to the farmers' practice for both experiments.

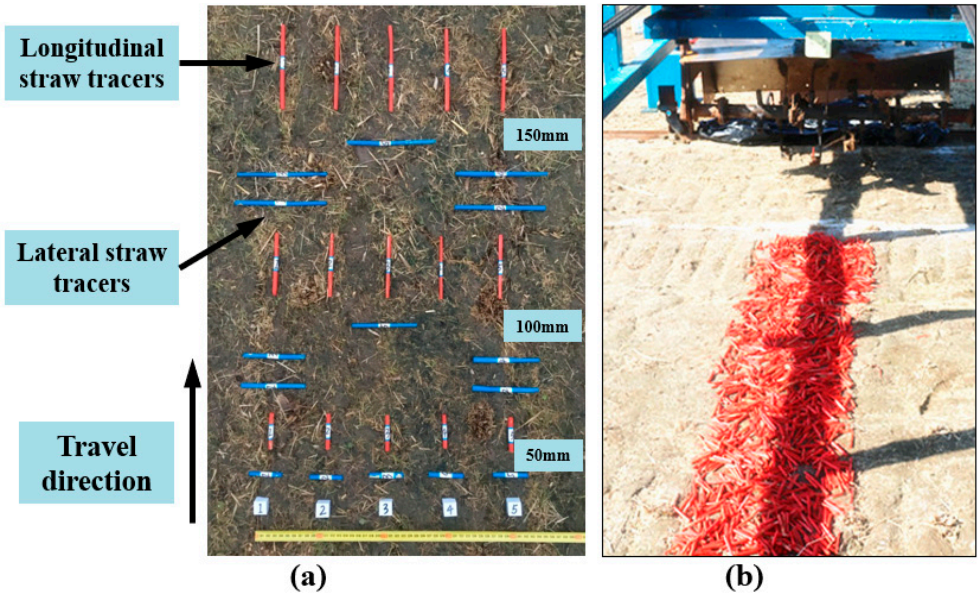

Figure 4. (**a**) Movement test: straw displacement test, (**b**) Tillage test: straw burying test.

2.5. Measurement

2.5.1. Straw Displacement

Straw displacements were recorded by documenting the alterations in the positions of tracers before and after tillage practices [26]. A label plate was inserted into the uncultivated soil surface as a reference line. The x and y coordinate values of straw tracers were determined by means of perpendicular rulers (Figure 5a), and the displacement value of the tracers was determined by calculating the absolute difference between the initial position and final positions of straw. The marked five red and five blue straws represent the longitudinal (tillage travel direction) straw and lateral (tillage width direction) straw, respectively. The straw displacement of all straw was represented by calculating the average value of five (5) sets of tracers. As the straw tracers may move in two dimensions (i.e., along the forward direction (tillage travel direction) and lateral direction (tillage width direction), straw tracers were measured in these two directions. The displacement of straw tracers was measured using the following relation [28]:

$$L = \sqrt{(x1 - x2)^2 + (y1 - y2)^2} \quad (1)$$

where x_i and y_i are coordinate values of straw tracers along the forward direction and lateral direction, respectively.

2.5.2. Straw Burying Rate

The straw burying rate is one of the important indexes to evaluate the quality of straw incorporation. The higher burying rate of straw implies a better quality of straw incorporation [12]. As shown in Figure 5b, to collect the quantity of straw on the soil surface after rotary tillage, a rectangular steel sampling frame with dimensions of 500 × 500 mm (used to keep the same area for each measurement) was positioned at the center of the tilled area, and then the exposed surface straws were removed with the help of a sampling frame and scissors. The total weight of straw in the sampling frame area was measured by an electronic scale. The straw burying rate was measured by using the following relation [10]:

$$Y = \frac{m_1 - m_2}{m_1} \times 100\% \quad (2)$$

where m_1 represents the total mass of straw (kg) before tillage and m_2 represents the total mass of surface straw (kg) after tillage.

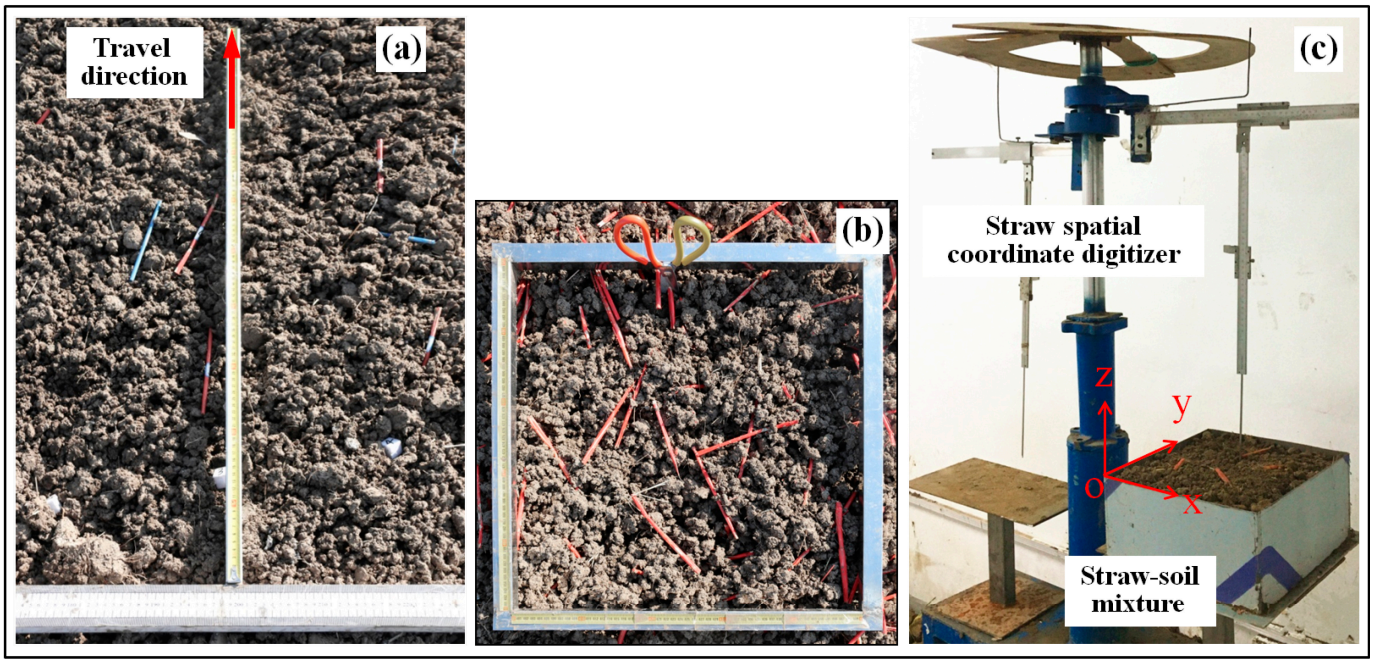

Figure 5. (**a**) Straw displacement measurement, (**b**) Straw burying measurement, (**c**) Straw distribution measurement.

2.5.3. Straw Distribution

To achieve the highest straw decomposition, straw should be evenly distributed in the soil and have complete contact between the straw and microorganisms. This, in turn, can reduce the input of chemical fertilizer in the field [29,30]. To obtain the data on straw distribution, a steel frame (300 × 300 × 150 mm) was used to collect the straw–soil mixture, and then a straw spatial coordinate digitizer was used to measure the straw spatial coordinates and create the 3D model of straw distribution (Figure 5c). The detailed process for sample collection and measurement of straw distribution, as well as 3D model reconstruction, was described in previous studies by the first author, Xu et al. [12].

In the depth direction, the model was segmented into three layers: the upper layer (UL), middle layer (ML), and lower layer (LL), and the proportion of total straw length in each layer was analyzed to evaluate the uniformity of straw distribution. A higher proportion of straw in LL indicates a more optimal straw distribution in the depth direction. In the overall direction, the model was further divided into 108 small cubes, and the coefficient of variation of total straw length (C_V) in each segment cube was analyzed to evaluate the uniformity of straw distribution. A small C_V means the better uniformity of straw distribution, and C_V was calculated using relation [31]:

$$CV = \frac{SD}{AV} \times 100\% \tag{3}$$

where SD is the standard deviation of total straw length and AV is the average value of total straw length.

2.5.4. Torque and Power

The torque and power of three tillage tools were obtained by a complete data acquisition system. As the tillage tool traveled in the soil, the system acquired data from all of the transducers at a suitable sampling frequency (100 samples per second), and the measurements were performed using Standard National Instruments Data Acquisition Card (SNIDAC) and Industrial Standard Software of LabVIEW 2020. After each test, the measured data were recorded on a computer hard disk for analysis.

2.6. Data Analysis

The data of straw displacement, straw burying rate, straw distribution, and torque and power among conventional, serrated, and biomimetic blades under different straw lengths were subjected to statistical analysis by one-way factorial analysis of variance (ANOVA) using IBM-SPSS Statistics 22 software (IBM Corp., Armonk, NY, USA). Duncan's multiple range tests were used to determine significance at a probability level of 0.05.

3. Results and Discussion

3.1. Straw Displacement

Figure 6 shows the straw displacement using conventional, serrated, and biomimetic blades under 50 mm, 100 mm, and 150 mm straw lengths. Straw displacement was 360 cm, 321 mm, and 285 mm; 327 mm, 274 mm, and 236 mm; 326 mm, 265 mm, and 228 mm using conventional, serrated, and biomimetic blades under 50 mm, 100 mm, and 150 mm straw lengths, respectively. Compared to conventional blades, the biomimetic blades recorded the lowest straw displacement under 50 mm, 100 mm, and 150 mm straw lengths. This may be possible due to the teeth of biomimetic and serrated blades, which pushed the straw backward with rotating blades in an ordered manner; there is no significant difference in straw displacement between biomimetic blades and serrated blades. Hence, biomimetic and serrated performed better than conventional blades for even distribution of straw in the soil.

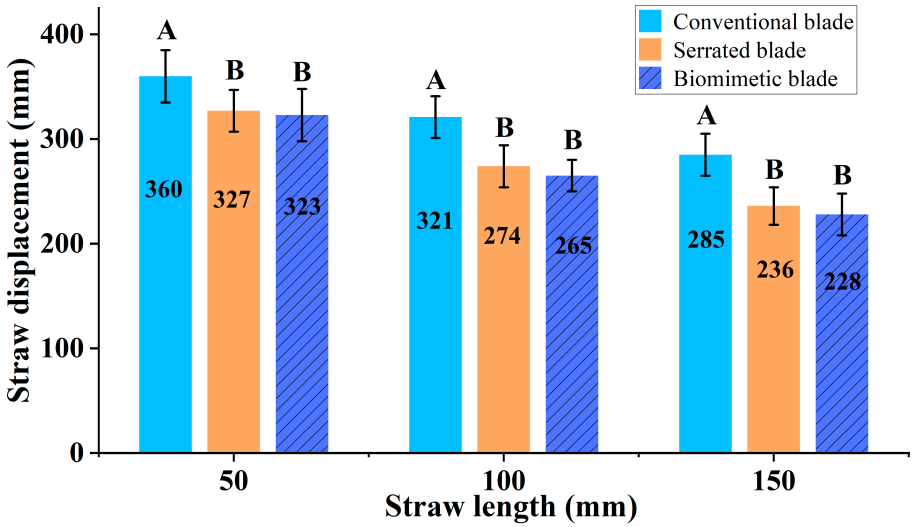

Figure 6. Straw displacement at three different blades under three different straw lengths. The means followed by different letters are significantly different according to Duncan's multiple range test at the significance level of 0.05; the error bars denote standard deviations (n = 3).

3.2. Straw Burying Rate

Figure 7 shows the straw burying rate using conventional, serrated, and biomimetic blades under 50 mm, 100 mm, and 150 mm. The straw burying rate was 87.7%, 81.6%, and 76.5%; 88.6%, 78.1%, and 71.3%; 91.4%, 87.3%, and 82.7% using conventional, serrated, and biomimetic blades under 50 mm, 100 mm, and 150 mm straw lengths, respectively. The highest straw burying rate was witnessed at the biomimetic blade, while the lowest was recorded at the serrated blade under 50 mm, 100 mm, and 150 mm straw lengths. Although the serrated blade yielded almost similar straw displacement to that of the biomimetic blade, it provided the lowest straw burying rate under all straw lengths. This may be attributable to the teeth of the serrated blade, which wrapped on the blade in the teeth gap, resulting in the lowest straw burying rate (Figure 8). Additionally, the longer straw was easier to wrap on the blade as compared to the shorter straw. The longer the length of the straw, the lower the straw burying rate. In contrast, the straw burying rate of the

biomimetic blade was 2.8%, 9.2%, and 11.4% more than the serrated blade at 50, 100, and 150 mm straw lengths, respectively, possibly due to the teeth of the biomimetic blade, which buried straw efficiently rather than winding on the blade. Therefore, the biomimetic blade could provide a better straw burying rate as compared to those of serrated and conventional blades.

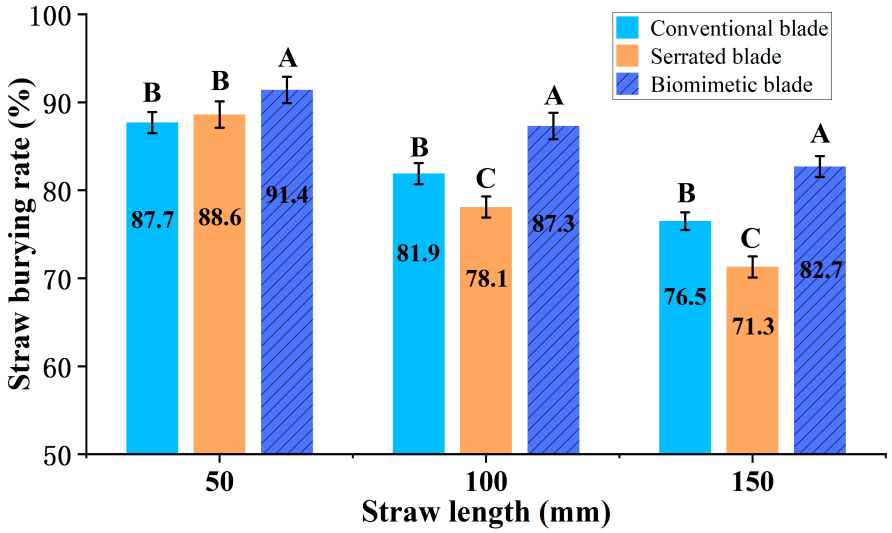

Figure 7. Straw burying rate at three different blades under three different straw lengths. The means followed by different letters are significantly different according to Duncan's multiple range test at the significance level of 0.05; the error bars denote standard deviations (n = 3).

Figure 8. The amount of straw wrapped around the frontal cutting edge of the three blades.

3.3. Straw Distribution

Table 3 shows the straw distribution at conventional, serrated, and biomimetic blades under 50 mm, 100 mm, and 150 mm in the depth direction. The proportion of straw in LL was 32.4%, 23.4%, and 12.7%; 32.3%, 17.9%, and 8.9%; 35.4%, 29.3%, and 20.5% using conventional, serrated, and biomimetic blades under 50 mm, 100 mm, and 150 mm straw lengths, respectively. And the corresponding total proportion of straw in UL and ML was 67.6%, 76.6%, and 87.3%; 67.7%, 82.1%, and 91.1%; 64.6%, 70.7%, and 79.5% using conventional, serrated and biomimetic blades, respectively. Compared to conventional and serrated blades, the biomimetic blades recorded the highest proportion of straw in LL under 50 mm, 100 mm, and 150 mm straw lengths. This may be associated with the teeth of biomimetic blades, due to which buried more straw into the lower layer of soil. Hence, it obtained better uniformity in straw distribution, which is conducive to the highest straw decomposition and crop emergence. In contrast, serrated blades recorded a 17.9% and 8.9% proportion of straw in LL under 100 and 150 mm straw lengths, respectively, while large straw was distributed in the UL. This would eventually result in hair pinning of straw

and blocking of the seed drills. Therefore, biomimetic blades provide maximum straw decomposition and crop emergence as compared to serrated and conventional blades.

Table 3. Straw distribution at three different blades in the depth direction.

Straw Length, mm	Layer, mm	The Total Length of Straw, mm			The Proportion of Straw, %		
		Conventional Blade	Serrated Blade	Biomimetic Blade	Conventional Blade	Serrated Blade	Biomimetic Blade
50	UL (0–50)	1274 ± 89	1231 ± 76	1081 ± 67	28.4	27.6	23.7
	ML (50–100)	1761 ± 121	1792 ± 134	1865 ± 129	39.2	40.1	40.9
	LL (100–150)	1458 ± 105	1445 ± 97	1617 ± 102	32.4	32.3	35.4
100	UL (0–50)	1676 ± 114	1850 ± 146	1504 ± 98	38.7	42.4	34.5
	ML (50–100)	1642 ± 93	1734 ± 105	1583 ± 81	37.9	39.7	36.2
	LL (100–150)	1017 ± 77	783 ± 56	1281 ± 72	23.4	17.9	29.3
150	UL (0–50)	2067 ± 148	2219 ± 154	1792 ± 133	47.3	50.8	41.1
	ML (50–100)	1743 ± 126	1761 ± 118	1674 ± 105	40.0	40.3	38.4
	LL (100–150)	556 ± 42	389 ± 41	895 ± 64	12.7	8.9	20.5

Note: UL is the upper layer; ML is the middle layer; LL is the lower layer.

Figure 9 shows C_V using conventional, serrated, and biomimetic blades under 50 mm, 100 mm, and 150 mm in the overall direction. The C_V was 68.1%, 77.5%, and 88.6%; 68.6%, 78.1%, and 91.3%; 62.1%, 67.8%, and 76.9% using conventional, serrated, and biomimetic blades under 50 mm, 100 mm and 150 mm straw lengths, respectively. The lowest C_V was witnessed using the biomimetic blade, while the highest was recorded with the serrated blade under 50 mm, 100 mm, and 150 mm straw lengths. The results indicated that the biomimetic design blade could improve the uniformity of straw distribution in soil, while the serrated design blade resulted in poor performance of straw distribution. This may be possible due to the wrapping of straw in the teeth gap of the serrated blade.

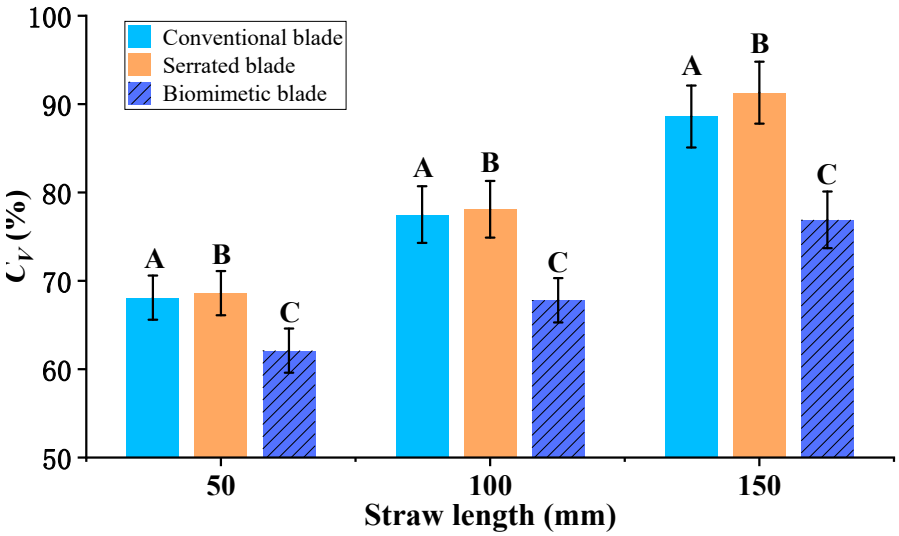

Figure 9. Straw distribution at three different blades in the overall direction. The means followed by different letters are significantly different according to Duncan's multiple range test at the significance level of 0.05; the error bars denote standard deviations (n = 3).

3.4. Torque and Power

Figure 10 shows the torque at conventional, serrated, and biomimetic blades under 50 mm, 100 mm, and 150 mm straw lengths. Torque was 44.7 N·m, 45.1 N·m, and 45.8 N·m; 44.6 N·m, 44.9 N·m, and 49.4 N·m; 41.6 N·m, 41.7 N·m, and 42.3 N·m using conventional, serrated and biomimetic blades under 50 mm, 100 mm, and 150 mm straw lengths, respectively. The highest torque was recorded using the serrated blade, while the lowest was

seen with the biomimetic blade under 50 mm, 100 mm, and 150 mm straw lengths. The biomimetic blade recorded 6.9%, 7.5%, and 7.6%; and 6.7%, 7.1%, and 14.4% less torque as compared to those of conventional and serrated blades under 50, 100, and 150 mm straw lengths, respectively. This may be possible due to the typical configurations of serrated and conventional blades.

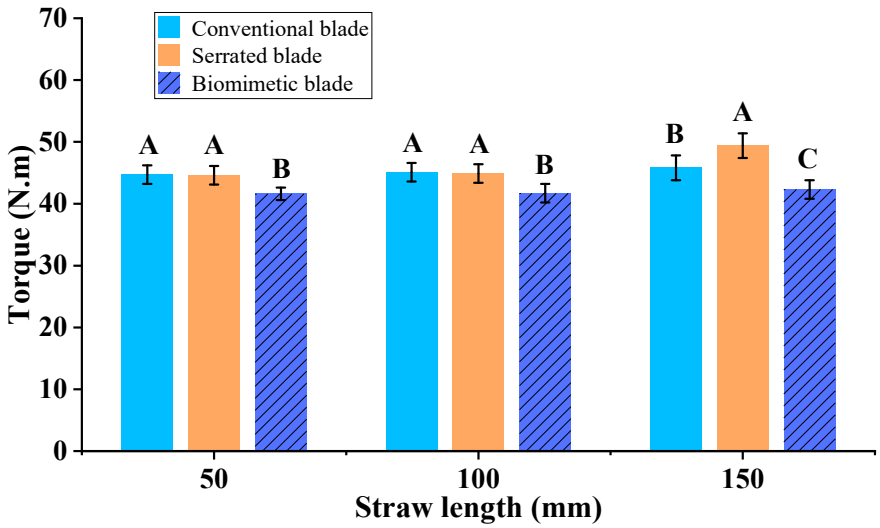

Figure 10. Torque at three different blades under three different straw lengths. The means followed by different letters are significantly different according to Duncan's multiple range test at the significance level of 0.05; the error bars denote standard deviations (n = 3).

A comparison of the PTO power for each test condition is shown in Table 4, showing the average power of the three blades at the three straw lengths. The average power was 1310.6 N·m, 1322.3 N·m, and 1342.8 N·m; 1307.6 N·m, 1316.4 N·m, and 1448.4 N·m; 1219.7 N·m, 1222.6 N·m, and 1240.2 N·m using conventional, serrated and biomimetic blades under 50 mm, 100 mm, and 150 mm straw lengths, respectively. Similar to torque, the highest average power was recorded using the serrated blade, while the lowest was seen with the biomimetic blade under 50 mm, 100 mm, and 150 mm straw lengths. Thus, the biomimetic blade could achieve lower torque and power as compared to serrated and conventional blades under all straw lengths.

Table 4. Average power of the three blades at the three straw lengths.

Straw Length, mm	Average Power, W		
	Conventional Blade	Serrated Blade	Biomimetic Blade
50	1310.6 ± 37.5 a	1307.6 ± 39.3 a	1219.7 ± 30.9 b
100	1322.3 ± 38.2 a	1316.4 ± 44.6 a	1222.6 ± 31.8 b
150	1342.8 ± 40.1 b	1448.4 ± 47.4 a	1240.2 ± 34.7 c

Means within a line followed by the same letters are not significantly different according to Duncan's multiple range test at the significance level of 0.05.

3.5. Discussion

3.5.1. Theory of Biomimetic Designed Toothed Blades as Straw Incorporation Tool

The kinematics of the straw can be assessed by assuming the force analysis. While tilling the soil with the conventional blade, most of the straw is not directly incorporated into the soil because it tends to slide out of the front cutting edge of the blade due to the high rotating speed of the blade, as illustrated in Figure 11a. This will eventually increase the energy consumption by repeated tillage operations. In contrast, the biomimetic-designed toothed blades could provide a highly efficient solution. As shown in Figure 11b, the biomimetic teeth moved the straw backward with the rotating blade and incorporated it

properly into the soil. As proposed by Fang et al. [13], optimizing the blade shape can improve the proportion of straw incorporated into the soil, which reduces the energy consumption during repeated tillage and increases the straw burying rate. Hence, a biomimetic-designed blade as a straw incorporation tool can not only reduce the tillage energy consumption but also improve the efficiency of straw incorporation.

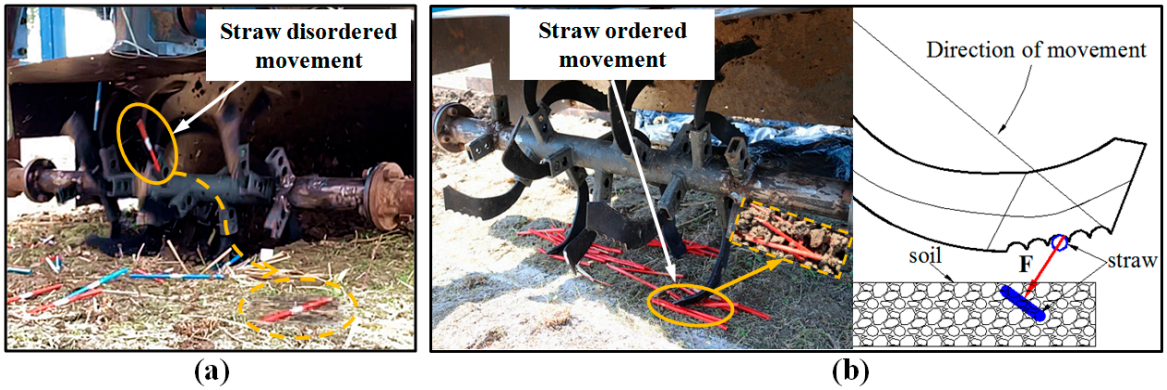

Figure 11. (**a**) Schematic view of straw disordered movement, (**b**) Schematic view of straw ordered movement.

3.5.2. Effect of Biomimetic-Designed Blades on the Performance of Straw Incorporation by Rotary Tillage

The present study indicated that it is feasible to achieve the desired tillage performance by using the biomimetic-designed blade for straw incorporation. The blade geometry significantly ($p < 0.05$) affected straw displacement, straw burying rate, straw distribution, and torque and power consumption. Compared to the conventional and serrated blades, the biomimetic blade had the lower straw displacement (decreased by an average of 50 mm and 7 mm, respectively), higher straw burying rate (increased by an average of 5.2% and 7.8%, respectively), better straw distribution (decreased by an average of 9.1% and 10.4% on the coefficient of variation, respectively), as well as lower torque and power (decreased by an average of 3.3 N·m and 4.4 N·m, respectively) under all straw lengths. The differences among the conventional, serrated, and biomimetic-designed blades can be attributed to the different configurations of blades.

Previous studies were mostly focused on the soil-cutting performance of biomimetic-designed blades [20,23,25], but a few were carried out on the straw movement based on the soil–straw–rotary blade interaction. By using the straw tracer method [32,33], we studied the straw movement characteristics for different rotary blades and realized the quantitative analysis of straw displacement. The present study found that the straw displacement was affected by the different rotary blades ($p < 0.05$), and the conventional blade had the larger straw displacement, while toothed blades (serrated and biomimetic blades) recorded the lower straw displacement. This is mainly due to the smooth edge of the conventional blade, which resulted in sliding over the straw and caused movement in a disordered manner. Toothed blades performed better due to the teeth, which caused the movement of straw backward in an ordered manner. This, in turn, reduced the straw displacement. Our study also found that the straw displacement decreased as straw length increased. This is consistent with Xu et al. [2], who reported that as the length of the straw increased from 50 mm to 150 mm, the straw displacement decreased from 279 mm to 224 mm. Eltom et al. [7] also stated that straw length had a significant impact on straw displacement. They further report that the straw displacement of long straw was less than that of short straw.

It was interesting to note that the straw burying rate of the serrated blade was lower than that of the conventional blade under higher straw lengths (i.e., 100 and 150 mm). On the contrary, Tong et al. [19] reported that toothed blades had a high straw-burying rate and straw-cutting efficiency. However, this was not true for our study, possibly due to the different soil and straw conditions. The rice straw has high toughness in Asian

rice–wheat fields. Hence, it was not cut with a toothed blade but rather wrapped around the teeth of the blades. Therefore, the serrated blade recorded a poor performance under high straw length. In contrast, the biomimetic blade showed better performance with little or no wrapping of straw due to its smooth arc teeth design. The biomimetic-designed blade moved the straw orderly with rotated blades, which in turn resulted in a high straw burying rate as compared to the conventional and serrated blades. The amount of straw wrapping around the tool also depends on soil and straw moisture content, which affects the adhesion between the straw and the tool. Further research is needed to determine the effect of teeth geometry on the straw wrapping phenomenon.

Many studies have explored straw incorporation performance of rotary blades [27,34]. Almost all studies to date have been focused on the single evaluation index of the straw burying rate. Although the straw burying rate could be used to compare the straw incorporation performance under different configurations of blades or operation parameters, the uniformity of straw distribution after tillage was not illustrated in these studies. In contrast, our study, for the first time, explored the effects of biomimetic-designed blades on the uniformity of straw distribution using three-dimensional software. It was found that compared to conventional and serrated blades, the biomimetic blades recorded the highest proportion of straw in LL and the lowest C_V under 50 mm, 100 mm, and 150 mm straw lengths.

Uniform incorporation of straw into the soil is beneficial to comprehensive contact between residues and microorganisms, leading to an augmentation of residue decomposition rates and a substantial reduction in the utilization of chemical fertilizers in the agricultural field [30,35,36].

It was also found that the blade designs had a significant effect ($p < 0.05$) on the torque and power. Compared to the conventional and serrated blades, the biomimetic blade had lower torque and power. This may be attributed to the low soil resistance of the teeth of biomimetic-designed blades, resulting in lower torque and energy consumption. This is consistent with Sun et al. [24], who found that the power and specific energy consumption of the bionic ditcher were lower than the traditional ditching blade, and the biotic-designed ditcher had the lowest resistance. Therefore, this study demonstrated that the biomimetic-designed blade offered a better straw burying rate and lower power consumption in Asian rice–wheat field conditions.

4. Conclusions

In intensive, high-yielding agriculture, agricultural practitioners have been searching for high-performance tillage tools to address the difficulties posed by dense straw conditions. We designed and developed a biomimetic blade by mimicking the claw profile of a mole-rat to improve and optimize the tillage performance. The performance of the biomimetic-designed blade was tested against conventional and serrated blades in rice-wheat fields in eastern China using an in situ test rig. This study has shown that a biomimetic-designed blade was found to be superior in achieving lower straw displacement, higher straw burying rate, better straw distribution, and lower torque and power under all straw lengths. Thus, the biomimetic-designed blade could be a better option for the proper incorporation of dense straw into the field conditions.

Author Contributions: Conceptualization, X.C. and G.X.; methodology, X.C. and G.X.; investigation, G.X.; writing—original draft preparation, X.C. and G.X.; writing—review and editing, X.C., G.X., X.Z., W.T., A.A.T., and Q.D.; visualization, X.C. and G.X.; funding acquisition, X.C and Q.D. All authors have read and agreed to the published version of the manuscript.

Funding: This research was funded by the National Key Research and Development Program of China (No. 2022YFD2300304), Key Research Platform and Project Number for Ordinary Universities in Guangdong Province (No. 2022ZDZX3089), and the Priority Academic Program Development of Jiangsu Higher Education Institutions (No. PAPD-2023-87).

Institutional Review Board Statement: Not applicable.

Informed Consent Statement: Not applicable.

Data Availability Statement: The original contributions presented in the study are included in the article; further inquiries can be directed to the corresponding author.

Conflicts of Interest: The authors declare no conflicts of interest.

References

1. Ittersum, V.; Martin, K. Crop yields and global food security. Will yield increase continue to feed the world? *Eur. Rev. Agric. Econ.* **2016**, *97*, 191–192. [CrossRef]
2. Xu, G.; Xie, Y.; Matin, M.A.; He, R.; Ding, Q. Effect of straw length, stubble height and rotary speed on residue incorporation by rotary tillage in intensive rice–wheat rotation system. *Agriculture* **2022**, *12*, 222. [CrossRef]
3. Liang, Z.; Wada, M.E. Development of cleaning systems for combine harvesters: A review. *Biosyst. Eng.* **2023**, *236*, 79–102. [CrossRef]
4. Zhou, M.; Wei, Z.; Wang, Z.; Sun, H.; Wang, G.; Yin, J. Design and experimental investigation of a transplanting mechanism for super rice pot seedlings. *Agriculture* **2023**, *13*, 1920. [CrossRef]
5. Ding, C.; Wang, L.; Chen, X.; Yang, H.; Huang, L.; Song, X. A blockchain-base wide-area agricultural machinery resource scheduling system. *Appl. Eng. Agric.* **2023**, *39*, 15332. [CrossRef]
6. Zeng, Z.; Chen, Y. Performance evaluation of fluted coulters and rippled discs for vertical tillage. *Soil. Till. Res.* **2018**, *183*, 93–99. [CrossRef]
7. Torotwa, I.; Ding, Q.; Makange, N.R.; Liang, L.; He, R. Performance evaluation of a biomimetically designed disc for dense-straw mulched conservation tillage. *Soil. Till. Res.* **2021**, *212*, 105068–105077. [CrossRef]
8. Eltom, A.F.; Ding, W.; Tagar, A.A.; Talha, Z.; Gamareldawla. Field investigation of a trash-board, tillage depth and low speed effect on the displacement and burial of straw. *Catena* **2015**, *133*, 385–393. [CrossRef]
9. Zhou, H.; Zhang, C.; Zhang, W.; Yang, Q.; Li, D.; Liu, Z.; Xia, J. Evaluation of straw spatial distribution after straw incorporation into soil for different tillage tools. *Soil. Till. Res.* **2020**, *196*, 104440. [CrossRef]
10. Fang, H.; Zhang, Q.; Chandio, F.A.; Guo, J.; Sattar, A.; Arslan, C.; Ji, C. Effect of straw length and rotavator kinematic parameter on soil and straw movement by a rotary blade. *Eng. Agric. Environ. Food* **2016**, *9*, 235–241. [CrossRef]
11. Shi, Y.; Xin, S.; Wang, X.; Hu, Z.; Newman, D.; Ding, W. Numerical simulation and field tests of minimum-tillage planter with straw smashing and strip laying based on EDEM software. *Comput. Electron. Agric.* **2019**, *166*, 105021. [CrossRef]
12. Xu, G.; Xie, Y.; Liang, L.; Alete, J.O.; Chen, X.; Abbas, A.; Matin, M.A.; He, R.; Ding, Q. A novel method for measuring and evaluating spatial distribution of straw incorporated by rotary tillage. *Agron. J.* **2022**, *114*, 853–866. [CrossRef]
13. Fang, H.; Niu, M.; Zhu, Z.; Zhang, Q. Experimental and numerical investigations of the impacts of separating board and anti-blocking mechanism on maize seeding. *J. Agric. Eng.* **2022**, *53*, 1–10.
14. Ahmad, F.; Qiu, B.; Ding, Q.; Ding, W.; Khan, Z.M.; Shoaib, M.; Chandio, F.A.; Rehim, A.; Khaliq, A. Discrete element method simulation of disc type furrow openers in paddy soil. *Int. J. Agric. Biol. Eng.* **2020**, *13*, 103–109. [CrossRef]
15. Jia, H.; Wang, W.; Wang, W.; Zheng, J.; Wang, Q.; Zhang, J. Application of anti-adhesion structure based on earthworm motion characteristics. *Soil. Till. Res.* **2018**, *162*, 34–40. [CrossRef]
16. Ren, L.Q.; Tong, J.; Li, J.Q.; Chen, B.C. Soil adhesion and biomimetics of soil-engaging components: A review. *J. Agric. Eng. Res.* **2001**, *79*, 239–263. [CrossRef]
17. Chirende, B.; Li, J. Review on application of biomimetics in the design of agricultural implements. *Biotechnol. Mol. Biol. Rev.* **2009**, *4*, 42–48.
18. Hu, J.; Xu, L.; Yu, Y.; Lu, J.; Han, D.; Chai, X.; Wu, Q.; Zhu, L. Design and experiment of bionic straw-cutting blades based on locusta migratoria manilensis. *Agriculture* **2023**, *13*, 2231. [CrossRef]
19. Tong, J.; Moayad, B.Z.; Ma, Y.; Sun, J.; Chen, D.; Jia, H. Effects of biomimetic surface designs on furrow opener performance. *J. Bionic Eng.* **2009**, *6*, 280–289. [CrossRef]
20. Ji, W.; Chen, D.; Jia, H.; Tong, J. Experimental investigation into soil-cutting performance of the claws of mole rat (*Scaptochirus moschatus*). *J. Bionic Eng.* **2010**, *7*, 166–171. [CrossRef]
21. Jia, H.; Wang, Q.; Huang, D.; Zhu, L.; Li, M.; Zhao, J. Design of bionic mole forelimb intelligent row cleaners. *Int. J. Agric. Biol. Eng.* **2019**, *12*, 27–35. [CrossRef]
22. Guan, C.; Fu, J.; Xu, L.; Jiang, X.; Wang, S.; Cui, Z. Study on the reduction of soil adhesion and tillage force of bionic cutter teeth in secondary soil crushing. *Biosyst. Eng.* **2020**, *213*, 133–147. [CrossRef]
23. Song, W.; Jiang, X.; Li, L.; Ren, L.; Tong, J. Increasing the width of disturbance of plough pan with bionic inspired subsoilers. *Soil. Till. Res.* **2022**, *220*, 105356. [CrossRef]
24. Sun, J.; Chen, H.; Wang, Z.; Ou, Z.; Yang, Z.; Liu, Z.; Duan, J. Study on plowing performance of EDEM low-resistance animal bionic device based on red soil. *Soil. Till. Res.* **2020**, *196*, 104336. [CrossRef]
25. Yang, Y.; Li, M.; Tong, J.; Ma, Y. Study on the interaction between soil and the five-claw combination of a mole using the discrete element method. *Appl. Bionics Biomech.* **2018**, *2018*, 7854052. [CrossRef]
26. Xu, G.; Xie, Y.; Liang, L.; Ding, Q.; Xie, H.; Wang, J. Straw-soil-rotary blade interaction: Interactive effects of multiple operation parameters on the straw movement. *Agronomy* **2022**, *112*, 847. [CrossRef]

27. Tong, J.; Ji, W.; Jia, H.; Chen, D.; Yang, X. Design and tests of biomimetic blades for soil-rototilling and stubble-breaking. *J. Bionic Eng.* **2015**, *12*, 495–503. [CrossRef]
28. Guo, J.; Ji, C.; Fang, H.; Zhang, Q.; Hua, F.; Zhang, C. Experimental analysis of soil and Straw displacement after up-cut and down-cut rotary tillage. *Trans. Chin. Soc. Agric. Eng.* **2016**, *47*, 21–26. (In Chinese)
29. Eagle, A.J.; Bird, J.A.; Hill, J.E.; Horwath, W.R.; van Kessel, C. Rice: Nitrogen dynamics and fertilizer use efficiency in rice following straw incorporation and winter flooding. *Agron. J.* **2001**, *93*, 1346–1354. [CrossRef]
30. Guan, X.; Wei, L.; Turner, N.; Ma, S.; Yang, M.; Wang, T. Improved straw management practices promote in situ straw decomposition and nutrient release, and increase crop production. *J. Clean. Prod.* **2020**, *250*, 119514.1–119514.13.
31. Chen, Q.; Shi, Y.; Ding, Q.; Ding, W.; Tian, Y. Comparison of straw incorporation effect with down-cut and up-cut rotary tillage. *Trans. Chin. Soc. Agric. Eng.* **2015**, *31*, 13–18. (In Chinese)
32. Zeng, Z.; Chen, Y. Simulation of straw movement by discrete element modelling of straw-sweep-soil interaction. *Biosyst. Eng.* **2019**, *180*, 25–35. [CrossRef]
33. Zeng, Z.; Ma, X.; Chen, Y.; Qi, L. Modelling residue incorporation of selected chisel ploughing tools using the discrete element method (DEM). *Soil. Till. Res.* **2020**, *197*, 104505. [CrossRef]
34. Ji, W.; Jia, H.; Tong, J. Experiment on working performance of bionic blade for soil-rototilling and stubble-breaking. *Trans. Chin. Soc. Agric. Eng.* **2012**, *28*, 24–30. (In Chinese)
35. Guérif, J.; Richard, G.; Dürr, C.; Machet, J.M.; Recous, S.; Roger-Estrade, J. A review of tillage effects on crop residue management, seedbed conditions and seedling establishment. *Soil. Till. Res.* **2001**, *61*, 13–32. [CrossRef]
36. Li, S.; Li, X.; Zhu, W.; Chen, J.; Tian, X.; Shi, J.; Kessel. Does straw return strategy influence soil carbon sequestration and labile fractions? *Agron. J.* **2019**, *111*, 1–10. [CrossRef]